be maintained by the ionosphere. The resulting slippage in the ionosphere heats the ionospheric electrons, producing high beta conditions along the entire flux tube.

Quite distinct from the waves surrounding the cavities was a 100-min-long burst of ion cyclotron waves (from 06:10 to 07:50 UT on 30 June 2004) unlike any seen on Voyager and Pioneer that appeared 5 hours after the Cassini engine stopped firing. These waves were limited to the frequency band expected for the singly ionized products of the engine exhaust H_2O, N_2, CO, and CO_2. We do not expect these waves to be present (except for H_2O^+ that may be associated with the icy satellites' environments) in the natural plasma. We note that Cassini's engine deposited over 850 kg of fuel in the Saturnian magnetosphere and, as it ionized and traversed the magnetosphere, it would produce a cloud of ions with energy predominantly transverse to the magnetic field, that is, a ring beam. The energy of these pickup ions at the locations where the waves were seen is comparable to that of the pickup ions in the Io torus. This may be the first detection of artificially induced plasma waves in a magnetosphere other than that of Earth.

References and Notes

1. M. K. Dougherty *et al.*, *Space Sci. Rev.* **114**, 331 (2004).
2. J. W. Dungey, *Phys. Rev. Lett.* **6**, 47 (1961).
3. International Astronomical Union standard definition of the Saturn equatorial body radius.
4. C. T. Russell, M. M. Hoppe, W. A. Livesey, *Nature* **296**, 45 (1982).
5. The ratio $\delta B/B0$ is the enhancement of the overshoot magnetic field normalized by the magnetosheath field strength away from the overshoot.
6. E. J. Smith *et al.*, *J. Geophys. Res.* **85**, 5655 (1980).
7. N. F. Ness *et al.*, *Science* **212**, 211 (1981).
8. N. F. Ness *et al.*, *Science* **215**, 558 (1982).
9. J. A. Slavin, E. J. Smith, P. Gazis, J. Mihalov, *Geophys. Res. Lett.* **10**, 9 (1983).
10. J. A. Slavin, E. J. Smith, J. Spreiter, S. Stahara, *J. Geophys. Res.* **90**, 6275 (1985).
11. C. M. Jackman *et al.*, *J. Geophys. Res.* **109**, A11203 (2004).
12. L. Davis, E. J. Smith, *J. Geophys. Res.* **95**, 15257 (1990).
13. M. H. Acuna, J. E. P. Connerney, N. F. Ness, *J. Geophys. Res.* **88**, 8771 (1983).
14. J. E. P. Connerney, M. H. Acuna, N. F. Ness, *J. Geophys. Res.* **88**, 8779 (1983).
15. G. Giampieri, M. K. Dougherty, *Geophys. Res. Lett.* **31**, 16701 (2004).
16. M. Schultz, M. C. McNab, *Geophys. Res. Lett.* **14**, 182 (1987).
17. N. A. Tsyganenko, *Planet. Space Sci.* **37**, 5 (1989).
18. N. A. Tsyganenko, *J. Geophys. Res.* **100**, 5599 (1995).
19. N. A. Tsyganenko, *J. Geophys. Res.* **107**, SMP12-1 (2002).
20. The dayside of the magnetopause is approximately ellipsoidal, but this is not the case in the tail, which is nearly circular in cross section. To accurately approximate the shape of the magnetopause, the tailward half of an ellipsoid is replaced with a cylinder; thus, the boundary is a composite surface composed of a hemi-ellipsoid and a cylinder. The join between these two surfaces is at the semi-minor axis of the prolate ellipsoid (nose portion).
21. E. J. Bunce, S. W. H. Cowley, J. A. Wild, *Ann. Geophys.* **21**, 1709 (2003).
22. E. J. Smith, B. T. Tsurutani, *J. Geophys. Res.* **88**, 7831 (1983).
23. C. T. Russell *et al.*, *Adv. Space Res.* **26**, 1489 (2000).
24. The KSM (Kronocentric Solar Magnetospheric) coordinate system has Saturn at the origin, with the $+X$ axis directed toward the Sun; Z defined such that Saturn's rotation and magnetic axis lies in the XZ plane (with $+Z$ pointing close to northward), and Y lying in Saturn's rotational and magnetic equatorial plane.
25. The reference for the SPV model is (*13*); for the Z3 model, (*14*); and the GD model, (*15*).

26. We wish to acknowledge the Cassini Project and operations team from the Jet Propulsion Laboratory, as well as the many people at our home institutions for their design, engineering, and software support over many years on behalf of this investigation. The contributions to the MAG team have been supported by the Particle Physics and Astronomy Research Council in the UK, Deutsches Zentrum für Luft-und Raumfahrt in Germany, and NASA in the U.S.

6 October 2004; accepted 7 December 2004
10.1126/science.1106098

REPORT

Dynamics of Saturn's Magnetosphere from MIMI During Cassini's Orbital Insertion

S. M. Krimigis,[1*] D. G. Mitchell,[1] D. C. Hamilton,[2] N. Krupp,[3] S. Livi,[1] E. C. Roelof,[1] J. Dandouras,[4] T. P. Armstrong,[5] B. H. Mauk,[1] C. Paranicas,[1] P. C. Brandt,[1] S. Bolton,[6] A. F. Cheng,[1] T. Choo,[1] G. Gloeckler,[2] J. Hayes,[1] K. C. Hsieh,[7] W.-H. Ip,[8] S. Jaskulek,[1] E. P. Keath,[1] E. Kirsch,[3] M. Kusterer,[1] A. Lagg,[3] L. J. Lanzerotti,[9,10] D. LaVallee,[1] J. Manweiler,[5] R. W. McEntire,[1] W. Rasmuss,[5] J. Saur,[1] F. S. Turner,[1] D. J. Williams,[1] J. Woch[3]

The Magnetospheric Imaging Instrument (MIMI) onboard the Cassini spacecraft observed the saturnian magnetosphere from January 2004 until Saturn orbit insertion (SOI) on 1 July 2004. The MIMI sensors observed frequent energetic particle activity in interplanetary space for several months before SOI. When the imaging sensor was switched to its energetic neutral atom (ENA) operating mode on 20 February 2004, at $\sim 10^3$ times Saturn's radius R_S (0.43 astronomical units), a weak but persistent signal was observed from the magnetosphere. About 10 days before SOI, the magnetosphere exhibited a day-night asymmetry that varied with an $\sim$11-hour periodicity. Once Cassini entered the magnetosphere, in situ measurements showed high concentrations of H^+, H_2^+, O^+, OH^+, and H_2O^+ and low concentrations of N^+. The radial dependence of ion intensity profiles implies neutral gas densities sufficient to produce high loss rates of trapped ions from the middle and inner magnetosphere. ENA imaging has revealed a radiation belt that resides inward of the D ring and is probably the result of double charge exchange between the main radiation belt and the upper layers of Saturn's exosphere.

The magnetosphere of Saturn was discovered by Pioneer 11 in 1979 (*1*, *2*) and was investigated in detail by Voyager 1 in 1980 (*3*) and Voyager 2 in 1981 (*4*). The primary science objectives of MIMI (*5*) are to determine the global configuration and dynamics of hot plasma in the magnetosphere of Saturn through energetic neutral particle imaging of the ring current, radiation belts, and neutral clouds; to study the sources of plasmas and energetic ions through in situ measurements of energetic ion composition, spectra, charge state, and angular distribution; to search for, monitor, and analyze magnetospheric spatial and time variations; to determine through imaging and composition studies the magnetosphere-satellite interactions at Saturn; to understand the formation of clouds of neutral hydrogen, nitrogen, and water products; and to study Titan's cometlike interaction with Saturn's magnetosphere and the solar wind. The MIMI instrument (*5*) comprises three sensors that measure particles in specific energy ranges: (i) the Ion and Neutral Camera (INCA), which measures ion and

[1]Applied Physics Laboratory, Johns Hopkins University, Laurel, MD 20723, USA. [2]Department of Physics, University of Maryland, College Park, MD 20742, USA. [3]Max-Planck-Institut für Sonnensystemforschung, D-37191 Lindau, Germany. [4]Centre D'Etude Spatiale Des Rayonnements, F-31028 Toulouse, France. [5]Fundamental Technologies Inc., Lawrence, KS 66049, USA. [6]Jet Propulsion Laboratory, Pasadena, CA 91109, USA. [7]Department of Physics, University of Arizona, Tucson, AZ 85721, USA. [8]Graduate Institute of Astronomy, National Central University, Jhongli City, Republic of China. [9]Bell Laboratories, Murray Hill, NJ 07974, USA. [10]New Jersey Institute of Technology, Newark, NJ 07102, USA.

*To whom correspondence should be addressed. E-mail: tom.krimigis@jhuapl.edu

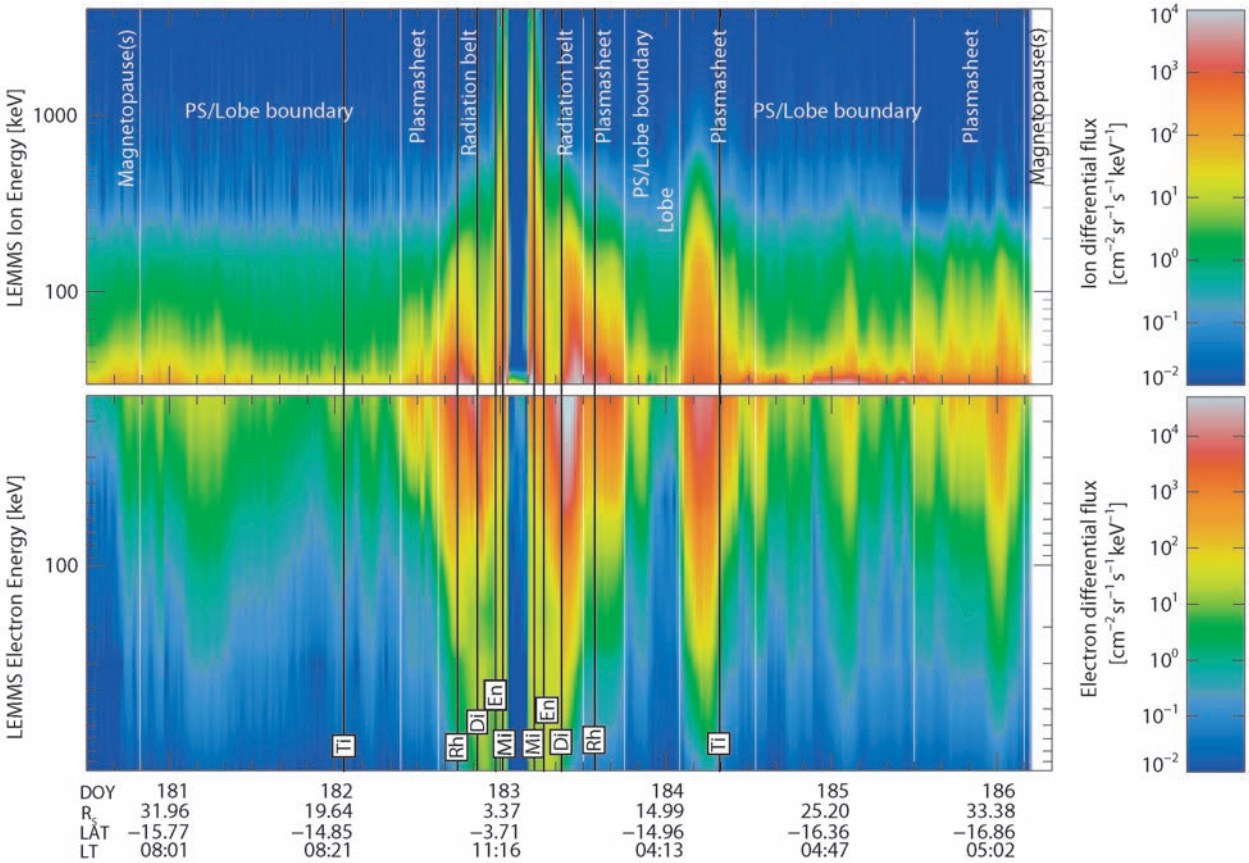

Fig. 1. Dynamic spectrograms (energy versus time) of LEMMS ion and electron intensities. Electron energy is plotted increasing downward for comparison with the features in the ion population. Magnetospheric regions are labeled and defined in the text. The general particle morphology is that of a well-defined radiation belt outside the ABC rings, transitioning abruptly to an extended, highly dynamic plasma sheet that extends outward to the magnetopause crossings (both inbound and outbound). Notations for moons: Ti, Titan; Rh, Rhea; Di, Dione; En, Enceladus; Mi, Mimas.

neutral species (~3 to 200 keV per nucleon); (ii) the Charge Energy Mass Spectrometer (CHEMS), which measures ions and their charge states (3 to 230 keV per charge); and (iii) the Low Energy Magnetospheric Measurement System (LEMMS), which measures ions (0.02 to 18 MeV) and electrons (0.015 to 1 MeV). LEMMS also measures high-energy electrons ($E > 3$ MeV) and protons ($1.6 < E < 160$ MeV) from the back end of the dual field-of-view telescope.

The LEMMS ion and electron intensities (Fig. 1) measured by MIMI in several magnetospheric regions during Cassini's inbound and outbound SOI pass (29 June to 4 July 2004) are similar to intensities measured by the Voyager 1 and 2 spacecraft (*3*, *4*). Measurements of the intensities and the magnetic field (*6*) allow us to define three different regions of the magnetosphere: the radiation belt, the plasma sheet, and the lobe. In general, the ions and electrons exhibit the same type of behavior. Essentially no energetic particles are detected above the rings, because they are effectively absorbed by solid material.

The radiation belt consists of energetic particles (tens to thousands of keV) with intensities that are locally modulated via absorption by saturnian satellites. Otherwise, ion and electron intensities generally exhibit smooth histories, although there are identifiable nondispersive intensity increases and decreases. The magnetic field strength and direction are consistent with those of a dipole (*6*). The highest ion and electron intensities (outside of the inner magnetosphere) are confined to the near-equatorial plasma sheet. Relatively abrupt increases in intensity occur as Cassini enters the plasma sheet region at the beginning of the plasma sheet intervals. Conversely, relatively abrupt decreases in intensity occur as Cassini leaves the plasma sheet region. Here the magnetic field is a stretched dipole with considerable irregular "noise" in the components (*6*). The lobe consists of significantly lower ion and electron intensities than in the plasma sheet and fewer ion/electron intensity variations (although these fluctuations seem to increase as Cassini moves beyond Titan's orbit). The field has a nearly radial orientation and less noise in field components, with Bz being the smallest component (SZS coordinates) (*6*). Frequent small nondispersive changes in ion and electron intensities are consistent with particle intensity gradients (away from the center of the plasma sheet) that are produced by small-scale plasma sheet flapping, thickening, or thinning.

The LEMMS measurements of ion and electron intensities are made in situ, so that temporal and spatial variations cannot be unambiguously distinguished from one another. However, the discovery of ENA emissions from Saturn by Voyager 1 (*7*) and at Earth (*8*) enabled a new approach. The INCA sensor is designed to provide a spatially resolved map of ENA emissions over a large region, similar to the IMAGE mission at Earth (*9*). An image taken at ~2200 UT on 2 July 2004 during Cassini's outbound pass reveals a day-to-night asymmetry in the emission of ENA (Fig. 2). In this image, INCA pointed toward Saturn for only a few hours, but during that time the emitting region corotated from the dayside to the nightside as it increased in brightness. The emission region extends beyond the orbit of Titan, as is also evident in the LEMMS measurements (Fig. 1). The nightside source varies with a time scale of ~11 hours, whereas the dayside seems relatively constant. Continuous measurements over longer periods show that an ~11-hour periodicity characterizes ENA emissions from the magnetosphere (*10*).

There are ENA emissions well off the limb of Saturn, emanating from the main radiation belt and extending tailward out to the edge of the instrument's field of view (Fig. 3A). There

Fig. 2. (**A**) ENA image of Saturn's magnetosphere obtained by INCA on 2 July 2004, 21:55 UTC (20 to 50 keV H, 4-hour integration). Cassini was moving below the ring plane, looking back and up at Saturn. The bright emission moves around the planet with the corotational speed (dashed line). (**B**) During the approach to Saturn (20–21 June), INCA revealed 11-hour variations in the ENA emissions coming from the magnetosphere of Saturn. The rotational period of Saturn is about 11 hours. The red and black curves show temporal variation of the summed ENA counts (3 to 80 keV H, 1-hour integration) on the dayside and nightside intensities, respectively. The differences in phase and intensity in the red and black curves imply that injected plasma clouds corotate.

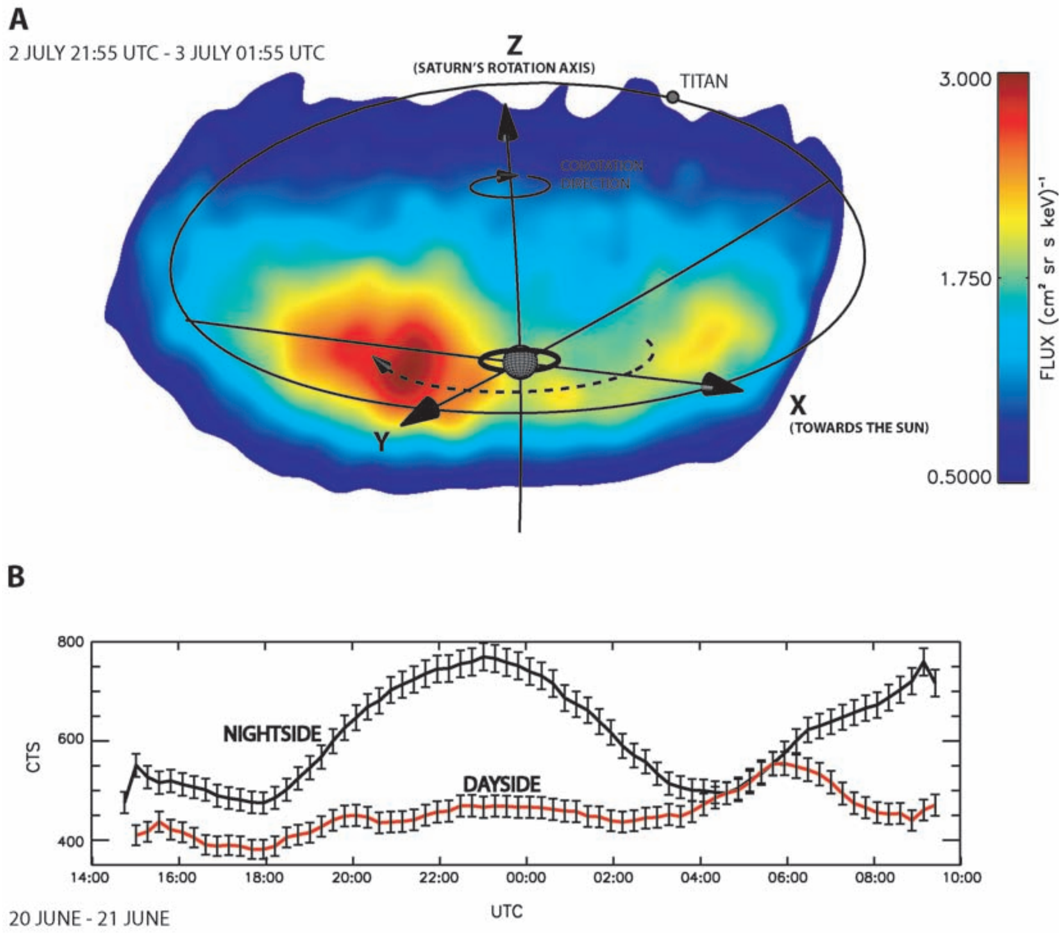

is also a high-intensity emission on Saturn's disk from a low-altitude equatorial belt. The ENA emission extends to a latitude 20° north of Saturn's equator. This equatorial emission originates as a belt inward of the innermost D ring, whereas the emission off the limb originates from the portion of the main radiation belt on the opposite side of Saturn (Fig. 3B).

The CHEMS instrument performed continuous measurements of the composition and charge state of ions throughout SOI, providing unique information on the likely origin of these accelerated ions in the magnetosphere. CHEMS data (Fig. 4) show that the principal constituents of the charged particle population are molecular and atomic ions, including H_2^+, O^{2+}, O^+, OH^+, H_2O^+, and O_2^+, most of which can originate as products of water dissociation. H^+ was abundant and could also originate from the dissociation of water or from Saturn's ionosphere or Titan's exosphere. He^+, which is abundant in interplanetary space (*11*), was also detected and probably enters the magnetosphere with relative ease. Most important, the relatively low concentration ($N^+/O^+ < 0.05$) of N^+—the most abundant element in Titan's atmosphere—suggests that little N_2 gas escapes from Titan's atmosphere, contrary to expectations (*12*, *13*).

The overall features of the energetic particle populations in the magnetosphere are similar to those observed during the Voyager 1 and 2 encounters more than two decades ago. There is a low-energy ion population associated with the dayside magnetopause extending inward to ~15 R_S [previously labeled "mantle" (*3*)], a rapid buildup in the intensity of ions and electrons just outside Rhea's L shell, a depletion of the ions and some electrons between the L shells of Dione and Enceladus inbound and outbound, and a rapid increase in the intensity of ions and electrons inside the orbit of Enceladus and Mimas (Fig. 1). The depletion of ions between the L shells of Dione and Enceladus suggests that the neutral gas that has been detected there for the past 6 months (*14*) may be the source for energetic particle loss through charge exchange. If so, a comparison of absolute fluxes between Cassini and Voyager data may allow us to determine the differences in neutral gas densities during the different spacecraft encounters.

Superimposed on the general morphology of the magnetosphere are some injections of plasma such as the one seen in the electrons on 2 July 2004, ~2030 UT (Fig. 1). Such injection events, characterized by energy dispersion (different energies arriving at the spacecraft at different times), have been observed in Earth's and Jupiter's magnetospheres (*15*). Injections are sudden planetward motions of hot plasma over a restricted range of longitudes and are a consequence of dynamical activity in planetary plasma environments such as in the magnetospheric substorm phenomenon. Conjectures about the existence of such injections in Saturn's magnetosphere were considered because of differences in intensities observed between the two Voyagers after successive encounters with Saturn in 1980 and 1981 (*16*).

The day-night asymmetry (Fig. 2) may be due to a larger accumulation of neutral gas on the nightside of Saturn. A maximum in particle intensity at some longitude corotating with the planet would produce more ENA on the nightside once per planetary rotation if the gas density were also maximized there. However, ENA production depends on the product of neutral gas density and particle intensity, so the excess emission could also be produced by higher nightside ion intensities. Constant particle intensity would result in bright ENA emission on the nightside but would not result in an 11-hour intensity variation of the nightside source (Fig. 2B). Hence, the interpretation of the 11-hour variation is not unambiguous at present.

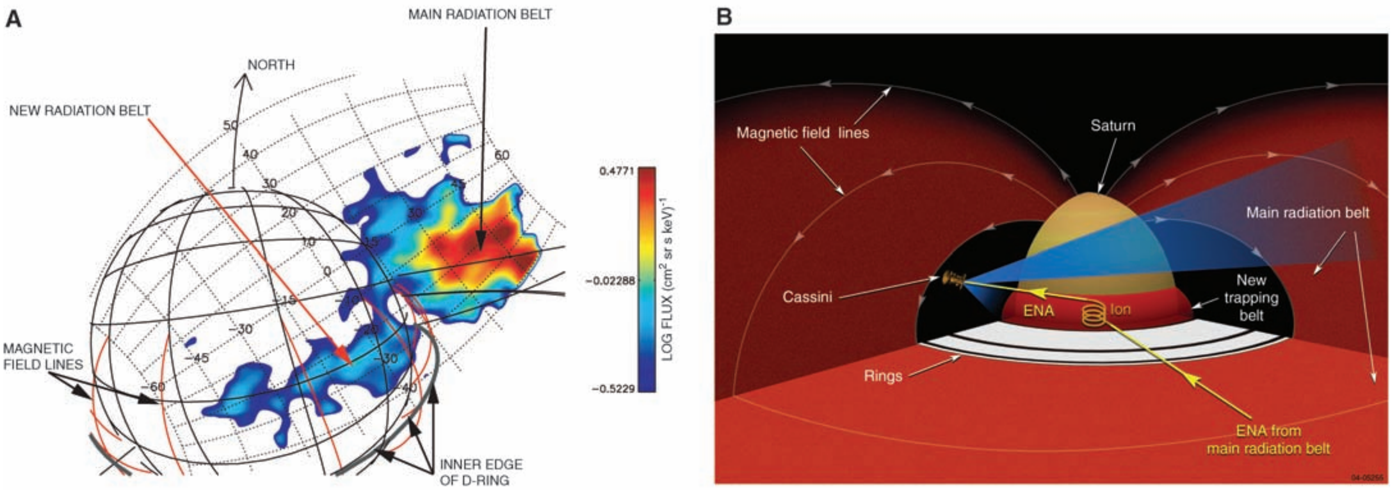

Fig. 3. ENA image obtained during Cassini's passage over the rings and interpretive schematic. (**A**) INCA image in 20 to 50 keV/nucleon ENAs. The bright region above Saturn's limb is caused by ENAs produced by charge-exchange collisions between main radiation belt ions and near-equatorial gas distributions. The band of emission above the equator on the disk is produced by the same ENAs from the main belt being stripped in Saturn's exosphere between the inner edge of the D ring and the cloud tops, trapped there temporarily as energetic ions, and then reemitted as ENAs that INCA can image. Note that the image is bounded by the limits of the INCA field of view (dotted arcs). (**B**) Schematic of the charge-exchange/stripping process that begins as ENA emission from the main belt and produces ENA emission from Saturn's exosphere.

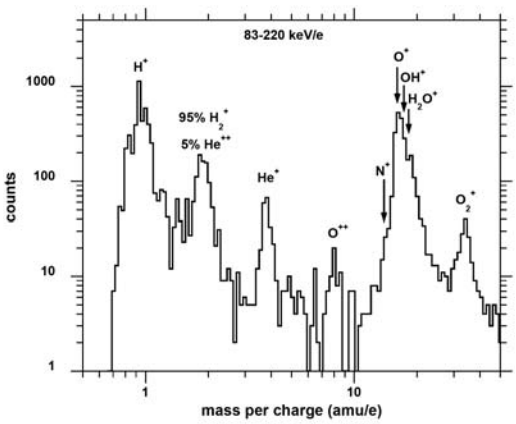

Fig. 4. Histogram of counts versus mass/charge ratios from MIMI and CHEMS, summed over the range 5.7 to 12.6 in the magnetic shell parameter L, during Cassini's outbound traversal (2 July 2004, 0800 to 1800 UTC) of the magnetosphere. The relative abundances are qualitatively correct. Although N^+ is not resolved in this display, fitting of the data shows an upper limit of $N^+/O^+ \approx 0.05$. At a mass/charge ratio of 2, the largest contribution is H_2^+ with a small amount (~5%) of He^{2+}.

The ENA-emitting region inward of the innermost D ring (Fig. 3) is explained as follows. The planet-directed ENAs from the main radiation belt are stripped of electrons when they enter Saturn's exosphere and are trapped as ions. However, the trapped ions will subsequently undergo a charge-exchange collision with exospheric atoms and be transformed back into ENAs. This process of stripping and charge exchange may be repeated many times, but some of these particles will eventually escape the exosphere as ENAs. Thus, a double charge-exchange process forms a low-altitude ENA emission region (Fig. 3B). A similar trapping belt was identified and explained by charge exchange in Earth's radiation belt (*17*) by in situ measurements at low altitudes. Although such a process at other planets might have been expected, none foresaw this happening at Saturn. Energetic particles, with their ability to pass back and forth between charged and neutral states, are temporarily unconstrained by (for instance) the Stoermer cutoff or ring absorption and therefore populate regions of space previously believed to be prohibited to them. The longitudinal extent of the inner belt has not been determined, but the ENA emission does extend all the way to the sunward edge of the INCA field of view. The ENA reemission process must be quite efficient, because the peak intensity of the low-altitude emission is about one-fifth of that from the main radiation belt.

Finally, the presence of a host of ions measured by CHEMS, apparently originating from H_2O, confirmed previous predictions (*16*, *18*) of abundant water products emanating from the rings and the icy satellites. The underlying chemistry has been described in the literature (*19*). The absence of significant amounts of N^+ ($\lesssim$5% of O^+) or N_2^+ is perplexing because N_2^+ was expected to be picked up by the magnetic field as it draped itself around Titan's exosphere (*12*, *20*). Molecular hydrogen could be a dissociation product of CH_4 in Titan's atmosphere, but the absence of nitrogen makes it more likely that the H_2^+ originated from water. H_2 at much higher energies was detected by Voyager and was thought to be escaping from Saturn's ionosphere (*3*, *4*). O_2^+ is not a direct dissociation product of water and may result from surface-gas reactions on ring particles.

References and Notes

1. J. A. Van Allen, M. F. Thomsen, B. A. Randall, R. L. Rairden, C. L. Grosskreutz, *Science* **207**, 415 (1980).
2. W. Fillius, W. H. Ip, C. E. McIlwain, *Science* **207**, 425 (1980).
3. S. M. Krimigis *et al.*, *Science* **212**, 225 (1981).
4. S. M. Krimigis *et al.*, *Science* **215**, 571 (1982).
5. S. M. Krimigis *et al.*, *Space Sci. Rev.* **114**, 233 (2004).
6. M. Dougherty *et al.*, *Science* **307**, 1266 (2005).
7. E. Kirsch, S. M. Krimigis, W. H. Ip, G. Gloeckler, *Nature* **292**, 718 (1981).
8. E. C. Roelof, D. G. Mitchell, D. J. Williams, *J. Geophys. Res.* **90**, 10991 (1985).
9. D. G. Mitchell *et al.*, *Geophys. Res. Lett.* **28**, 1151 (2001).
10. S. M. Krimigis *et al.*, 36th Division of Planetary Sciences Meeting, Louisville, KY, 8 to 12 November 2004.
11. G. Gloeckler *et al.*, in *The Heliosphere Near Solar Minimum*, A. Balogh, R. G. Marsden, E. J. Smith, Eds. (Springer-Praxis, Chichester, UK, 2001), pp. 287–326.
12. A. Eviatar, M. Podolak, *J. Geophys. Res.* **88**, 833 (1983).
13. J. D. Richardson, *Rev. Geophys.* **36**, 501 (1998).
14. L. Esposito *et al.*, *Science* **307**, 1251 (2005).
15. B. H. Mauk, D. J. Williams, R. W. McEntire, K. K. Khurana, J. G. Roederer, *J. Geophys. Res.* **104**, 22759 (1999).
16. S. M. Krimigis *et al.*, *J. Geophys. Res.* **88**, 8871 (1983).
17. J. Moritz, *Z. Geophys.* **38**, 701 (1972).
18. A. F. Cheng, S. M. Krimigis, in *Outstanding Problems in Solar System Plasma Physics: Theory and Instrumentation*, J. H. Waite, R. Moore, Eds. (American Geophysical Union, Washington, DC, 1989), pp. 253–260.
19. W. H. Ip, *Adv. Space Res.* **12**, 73 (1992).
20. H. T. Smith, R. E. Johnson, V. I. Shematovich, *Geophys. Res. Lett.* **31**, L16804 (2004).
21. The MIMI program at the Applied Physics Laboratory, Johns Hopkins University, was supported by the NASA Office of Space Science under Task Order 003 of contract NAS5-97271 between the NASA Goddard Space Flight Center and Johns Hopkins University and by subcontract at the universities of Maryland, Kansas, and Arizona.

4 October 2004; accepted 30 November 2004
10.1126/science.1105978

Dynamics of Saturn's Magnetosphere from MIMI During Cassini's Orbital Insertion

S. M. Krimigis, D. G. Mitchell, D. C. Hamilton, N. Krupp, S. Livi, E. C. Roelof, J. Dandouras, T. P. Armstrong, B. H. Mauk, C. Paranicas, P. C. Brandt, S. Bolton, A. F. Cheng, T. Choo, G. Gloeckler, J. Hayes, K. C. Hsieh, W.-H. Ip, S. Jaskulek, E. P. Keath, E. Kirsch, M. Kusterer, A. Lagg, L. J. Lanzerotti, D. LaVallee, J. Manweiler, R. W. McEntire, W. Rasmuss, J. Saur, F. S. Turner, D. J. Williams and J. Woch

Science **307** (5713), 1270-1273.
DOI: 10.1126/science.1105978